ANTIOXIDANTS & REDOX SIGNALING
Volume 22, Number 2, 2015

DOI: 10.1089/ars.2013.5595

FORUM ORIGINAL RESEARCH COMMUNICATION

Antihelminthic Benzimidazoles Are Novel HIF Activators That Prevent Oxidative Neuronal Death *via* Binding to Tubulin

Hossein Aleyasin,[1,2,*] Saravanan S. Karuppagounder,[1,2,*] Amit Kumar,[1,2] Sama Sleiman,[1,2] Manuela Basso,[1,2] Thong Ma,[1,2] Ambreena Siddiq,[1,2] Shankar J. Chinta,[3] Camille Brochier,[1,2] Brett Langley,[1,2] Renee Haskew-Layton,[1,2] Susan L. Bane,[4] Gregory J. Riggins,[5] Irina Gazaryan,[1,2] Anatoly A. Starkov,[2] Julie K. Andersen,[3] and Rajiv R. Ratan[1,2]

Abstract

Aims: Pharmacological activation of the adaptive response to hypoxia is a therapeutic strategy of growing interest for neurological conditions, including stroke, Huntington's disease, and Parkinson's disease. We screened a drug library with known safety in humans using a hippocampal neuroblast line expressing a reporter of hypoxia-inducible factor (HIF)-dependent transcription. ***Results:*** Our screen identified more than 40 compounds with the ability to induce hypoxia response element-driven luciferase activity as well or better than deferoxamine, a canonical activator of hypoxic adaptation. Among the chemical entities identified, the antihelminthic benzimidazoles represented one pharmacophore that appeared multiple times in our screen. Secondary assays confirmed that antihelminthics stabilized the transcriptional activator HIF-1α and induced expression of a known HIF target gene, $p21^{cip1/waf1}$, in post-mitotic cortical neurons. The on-target effect of these agents in stimulating hypoxic signaling was binding to free tubulin. Moreover, antihelminthic benzimidazoles also abrogated oxidative stress-induced death *in vitro*, and this on-target effect also involves binding to free tubulin. ***Innovation and Conclusions:*** These studies demonstrate that tubulin-binding drugs can activate a component of the hypoxic adaptive response, specifically the stabilization of HIF-1α and its downstream targets. Tubulin-binding drugs, including antihelminthic benzimidazoles, also abrogate oxidative neuronal death in primary neurons. Given their safety in humans and known ability to penetrate into the central nervous system, antihelminthic benzimidazoles may be considered viable candidates for treating diseases associated with oxidative neuronal death, including stroke. *Antioxid. Redox Signal.* 22, 121–134.

Introduction

HYPOXIA IS A fundamental, primordial stress endured by cells for billions of years. Understanding the molecular mechanism by which metazoans adapt to hypoxia has opened the door to new therapeutic strategies that combat hypoxic insults, including those involving ischemia. Hypoxia-inducible factor (HIF)-1 is a heterodimeric transcription factor composed of a hypoxia-regulated HIF-1α subunit and a constitutive HIF-1β subunit (21, 56, 59). It has been identified as one of the key molecular players of different adaptive responses to hypoxia. This heterodimer can mediate the expression of more than 100 genes involved in cellular, local, and systemic adaptation to a discrepancy in oxygen demand and supply (31, 46).

Under normoxia, in each cell of the body, including neurons and astrocytes, HIF-1α is constitutively transcribed and translated into protein. A set of HIF prolyl hydroxylases (HIF-PHDs) destabilizes HIF-1α in normoxia by hydroxylating it at proline 402 and proline 564. HIF prolyl hydroxylation targets

[1]Burke-Cornell Medical Research Institute, White Plains, New York.
[2]Department of Neurology and Neuroscience, Weill Medical College of Cornell University, New York, New York.
[3]Buck Institute for Age Research, Novato, California.
[4]Department of Chemistry, State University of New York at Binghamton, Binghamton, New York.
[5]Department of Neurosurgery, Johns Hopkins University School of Medicine, Baltimore, Maryland.
*These two authors contributed equally.

Innovation

By screening a hypoxia-inducible factor (HIF) reporter expressed in a hippocampal neuroblast line against a library of clinically approved drugs, we have defined antihelminthic benzimidazoles as novel inducers of the transcriptional adaptive response to hypoxia in neurons. In contrast to cancer cells where tubulin-binding drugs inhibit HIF activation, we have shown that the on-target effect of these drugs in activating hypoxic adaptation and protecting from oxidative neuronal death is free β-tubulin. Altogether, these results define a novel target for manipulating adaptive transcriptional responses in neurons and preventing oxidative death. Since antihelminthic benzimidazoles are utilized around the world for treatment of parasitic infections, our findings suggest that they could be employed readily in humans as hypoxia mimics and to treat brain injury associated with oxidative stress.

HIF-1α for recruitment and polyubiquitination by the Von Hippel-Lindau (VHL) E3 Ubiquitin ligase complex, leading to degradation by the proteasome (8, 21). Under conditions of hypoxia, the HIF-PHDs cease to function, and HIF-1α is, thus, not hydroxylated and degraded. The stabilized HIF-1α dimerizes with its partner, HIF-1β, translocates to the nucleus, and induces expression of a host of genes, including erythropoietin (EPO) and vascular endothelial growth factor (VEGF), both of which are neuroprotective (14, 18, 38, 41). Since the identification of this adaptive response, a number of groups, including our own, have established that activators of the HIF pathway are neuroprotective, especially those targeting HIF-PHDs (27, 35, 37, 40, 50).

To identify novel activators of the HIF pathway in neurons with known safety in humans, we stably transfected a hypoxia response element (HRE) upstream of a luciferase reporter (HRE-Luc) in immortalized hippocampal neuroblasts. We subsequently screened these cells against a library of 1040 FDA-approved compounds, including drugs, nutriceuticals, and reference chemicals from MicroSource Spectrum Collection (Microsource Discovery, Inc.). Here, we describe the results of our screen and the identification of antihelminthic benzimidazoles as unexpected activators of the host adaptive response to hypoxia in neurons *in vitro* and in the brain *in vivo*. Since these compounds are extensively used in clinical practice, our findings suggest they could be interesting pharmacological candidates for the treatment of neurological conditions involving oxidative or hypoxic stress.

Results

Identification of FDA-approved activators of hypoxic adaptive response

To screen for activators of HIF-mediated transcription, we used a luciferase promoter-reporter construct driven by a 68 bp region of enolase promoter containing a wild type HRE (HRE-Luc) stably expressed in immortalized hippocampal neuroblasts (HT22-HRE) (Fig. 1A). We have previously shown that enolase is upregulated by hypoxia or deferoxamine (DFO) in primary cortical neurons at both mRNA and protein levels, and validated the reporter by showing that DFO (10 μM) induces a nearly twofold increase in luciferase activity in HT22 cells transiently transfected with HRE-Luc. Importantly, mutations in the HRE sequence abrogated the response to DFO, while mutations outside the HRE did not affect DFO-induced reporter activity (1, 61).

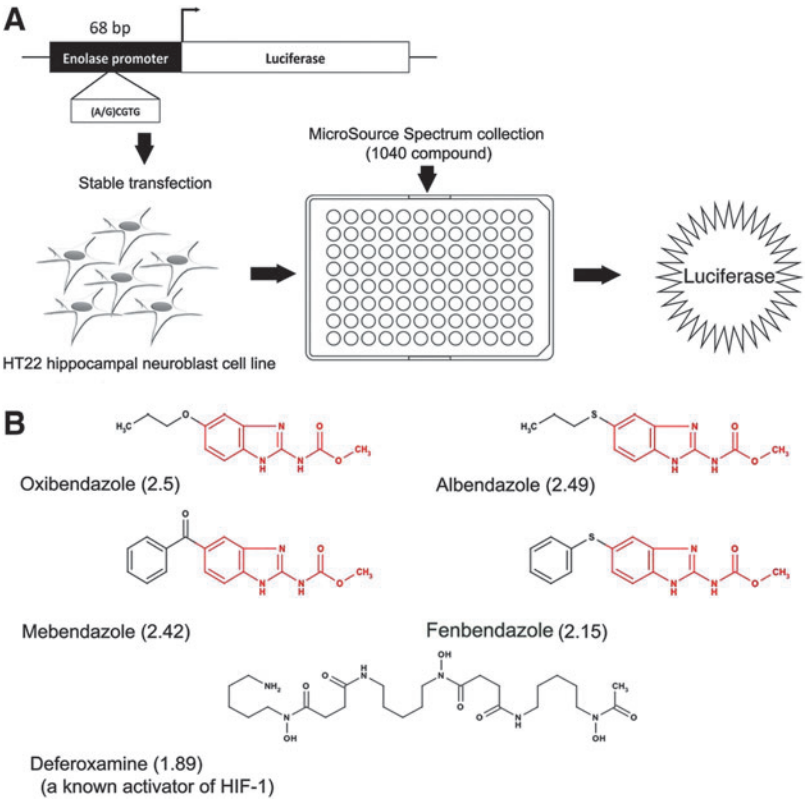

FIG. 1. Large-scale screening for activators of HIF-dependent gene expression identifies several pharmacophores, including the antihelminthic benzimidazoles. (A) Schematic representation of screening of MicroSource Spectrum collection of 1040 FDA-approved drugs and small molecules using a luciferase reporter driven by 68 bp of a canonical HIF-1-regulated gene promoter (enolase) containing the HRE, stably expressed in HT22 cells. **(B)** Chemical structures of benzimidazoles and DFO, a canonical activator of hypoxic adaptive response. The benzimidazole pharmacophore is represented in *red*. The average increase of luciferase signal for each compound is shown in *parentheses*, as fold increase over control. DFO, deferoxamine; HIF, hypoxia-inducible factor; HRE, hypoxia response element. To see this illustration in color, the reader is referred to the web version of this article at www.liebertpub.com/ars

To identify inducers of HRE-dependent transcription with known safety in humans, we screened the 1040 compound Microsource Library Collection using the HRE-Luc-expressing HT22 cells. Each compound was added to cells in 96-well plates at a final concentration of 10 μM, including DFO as a positive control. Luciferase activity was normalized to cell viability in each well as measured by MTT assay. Using this strategy, we identified a number of known activators of the HIF pathway, including the anti-viral agent tilorone (45), the antifungal ciclopirox (28, 53), and the antihypertensive hydralazine (23), which validates our screening tools (Table 1). Of note, the antihelminthic benzimidazoles, a group of structurally similar compounds, show multiple hits: oxibendazole (2.5-fold), mebendazole (2.42-fold), albendazole (2.49-fold), and fenbendazole (2.15-fold). Interestingly, each drug induced a greater degree of HRE activity than DFO (1.89-fold at 10 μM) (Fig. 1B).

Table 1. Drugs That Activate HRE-Luc Reporter

Name	*Fold increase*
Known HIF activators	
Tilorone	9.76
Ciclopiroxolamine	2.99
Deferoxaminemesylate	1.89
Hydralazine	1.61
Antihelminthics	
Oxibendazole	2.5
Albendazole	2.49
Mebendazole	2.42
Fenbendazole	2.15
NSAIDs	
Indoprofen	4.18
Nabumetone	2.69
Zomepirac sodium	2.19
Ibuprofen	1.89
Antibiotics	
Monesin sodium	2.41
Clofoctol	2.31
Trimethoprim	2.05
Clindamycin hydrochloride	1.99
Sulfachlorpyridazine	1.98
Nafcillin sodium	1.86
Anabolic isoflavones	
Methoxyisoflavone (7-methoxy-5-methyl-2-phenyl-chromen-4-one)	2.37
Ipraflavone or ipriflavone	2.32
Biochanin A	2.19
Daidzein	2.11
Antihistamines	
Hydroxyzine pamoate	2.36
Triprolidine hydrochloride	2.12
Tripelennamine citrate	2.09
Antineoplastics	
Helenaline	2.03
Hydroxyurea	2.02
Semustine	1.94
Channel blockers and neuroreceptor modulators	
Tropicamide	2.47
Pramoxine hydrochloride	2.46
Atenolol	2.43
Xylometazoline	2.18
Pirenzepine hydrochloride	2.15
Aminopyridine	2.08
Amiodarone hydrochloride	1.99
Mephenesin	1.97
Hyoscyamine	1.86
Clidinium bromide	1.80
Miscellaneous	
Tryptophan	2.87
Anisindione	2.69
Carbetapentane citrate	2.42
Phenazopyridine hydrochloride	2.36
Colchicine	2.08
Clofibric acid	1.91
Piperin	1.84
Trioxsalen	1.8

HIF, hypoxia-inducible factor.

Benzimidazoles stabilize HIF-1α and induce HIF-regulated gene transcription

HIF-1α stability is primarily governed by HIF-PHDs, which in the presence of oxygen hydroxylate HIF-1α within its oxygen-dependent degradation domain (ODD). To establish whether albendazole and fenbendazole interfere with HIF-PHD-regulated pathways, we tested these agents with a reporter containing the HIF-1α ODD fused to luciferase (ODD-Luc). The ODD-luc construct encoded in pcDNA3.1 plasmid vector was constructed as previously described (47). Both albendazole and fenbendazole increased ODD-Luc activity in a concentration-dependent manner in HT22 cells (Fig. 2A), while having no effect on a constitutive cytomegalovirus (CMV) luciferase construct (not shown). HRE activation customarily results from stabilization of HIF-1α followed by binding of a HIF-1α/HIF-1β heterodimer to the HRE. To establish whether increased activity of HRE-Luc reporter by benzimidazoles reflects the stabilization of HIF-1α protein in HT22 cells, we performed immunoblots using an antibody specific for HIF-1α. As a positive control, we used a 100 μM DFO, which was 10-fold higher than our screening dose of benzimidazoles. For validation purposes, we used albendazole and fenbendazole, two agents commonly applied in clinical practice in humans and animals. As shown in Figure 2B, they induce HIF-1α protein at the screening dose (10 μM) in HT22 cells.

These findings suggest that benzimidazoles are interdicting an aspect of canonical oxygen-dependent signaling. To verify these results in post-mitotic neurons, we treated primary mouse cortical neurons with albendazole and fenbendazole, and found that each induced mRNA levels of $p21^{cip1/waf1}$ (*p21*), an established HIF-1-regulated gene (Fig. 2C). As expected, albendazole and fenbendazole also increased p21 protein levels (Fig. 2D). Together, these data suggest that benzimidazoles induce HIF stability *via* a canonical HIF-PHD-regulated mechanism, resulting in increased HIF-dependent gene expression.

Benzimidazoles do not regulate HIF activity through inhibition of mitochondrial function

To understand how benzimidazoles might stabilize HIF, we focused on their known activity in killing parasites. One possibility is having global effects on mitochondrial function. To investigate the global effects on mitochondrial function, we measured mitochondrial membrane potential, oxygen

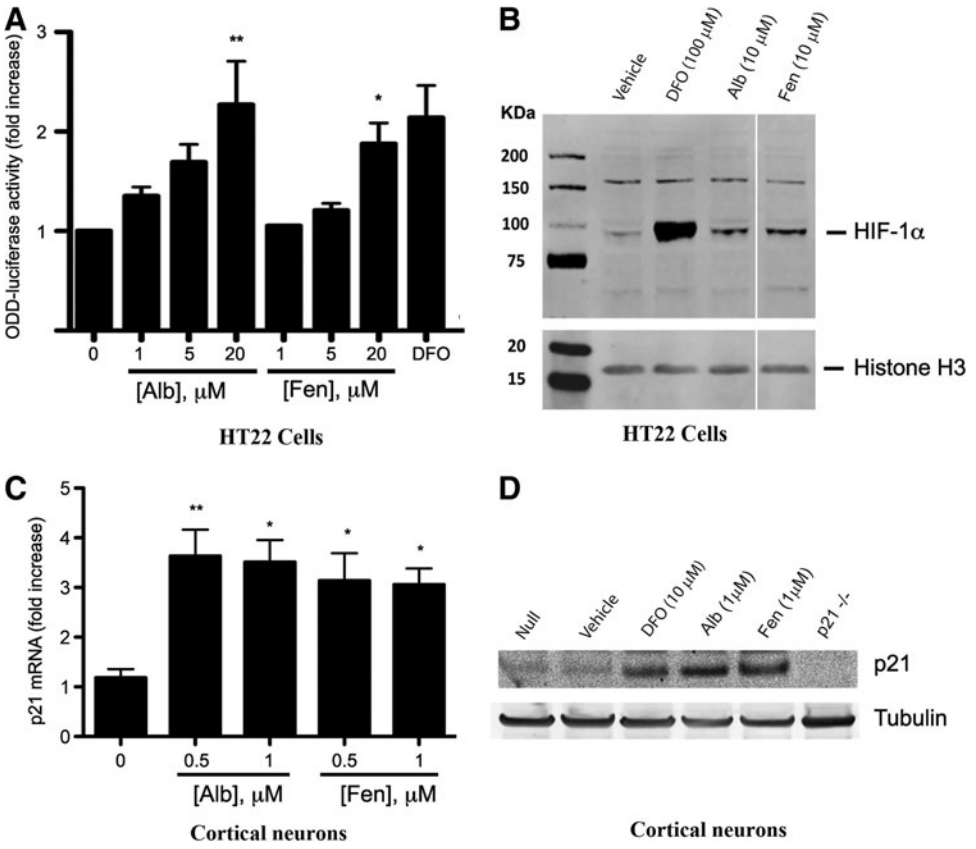

FIG. 2. Secondary screens confirm activation of adaptive responses to hypoxia by benzimidazoles. (A) Quantification of changes in an ODD-Luciferase activity, at 4 h after treatment with indicated doses of albendazole (Alb), fenbendazole (Fen), and vehicle in HT22 cells stably transfected with ODD-Luc construct. DFO, 100 μM was used as a positive control. **(B)** Immunoblot analysis shows HIF-1α stabilization in HT22 cells at 4 h after treatment with DFO (100 μM, as a positive control), vehicle (Veh), albendazole (Alb), or fenbendazole (Fen). The band stabilized was verified to be HIF-1α using siRNA-mediated knockdown (not shown). **(C)** Real-time polymerase chain reaction results show that mRNA levels of $p21^{cip1/waf1}$ (*p21*), an HIF-regulated gene, is upregulated by benzimidazoles in cultured embryonic cortical neurons at 8 h after treatment with select benzimidazoles compared with vehicle. **(D)** Immunoblot of proteins from cultured cortical neurons non-treated (Null), or treated with indicated doses of DFO (10 μM) and benzimidazoles (1 μM) using a *p21* antibody shows an increased $p21^{cip1/waf1}$ level at 20 h after treatment. Protein extract from $p21^{cip1/waf1}$ null ($p21^{-/-}$) cortical neurons was run as a negative control. Quantifications of results are presented as the mean of three independent experiments ± SEM (*$p < 0.05$, **$p < 0.01$, one-way ANOVA with Dunnett multiple-comparison test). ANOVA, analysis of variance; ODD, oxygen-dependent degradation domain; SEM, standard error of mean.

consumption rate, and reactive oxygen species (ROS) production in isolated mitochondria and found that these parameters were unchanged by exposure to benzimidazoles (Fig. 3). A second mechanism is the inhibition of worm mitochondrial enzymes, such as fumarase, that results in energy depletion (33). In mitochondria, fumarase participates in the tricarboxylic acid (TCA) cycle and is essential for oxidative ATP synthesis. Inhibition of fumarase in worms can lead to mitochondrial dysfunction, immobilization, and death of the parasite (42). In humans, activity-inhibiting mutations of fumarase lead to an accumulation of fumarate and succinate in the cytoplasm and mitochondria. These metabolites are proposed to promote HIF-1α stability by inhibiting HIF-PHDs through competition with 2-oxoglutarate, a necessary cofactor for prolyl hydroxylase activity (17, 48). To determine whether benzimidazoles stabilize HIF-1α by inhibiting a TCA cycle enzyme, we measured the effect of benzimidazoles on fumarase activity. We found that of the four benzimidazoles tested, only mebendazole inhibited fumarase activity (Supplementary Fig. S1A; Supplementary Data are available online at www.liebertpub.com/ars). However, this occurs at concentrations that are 30-fold higher than those used in our screen (10 μM) (Supplementary Fig. S1B). Similarly, the enzyme activities of mitochondrial citrate synthase and malonyl dehydrogenase were unchanged by these benzimidazoles (data not shown). Based on these results, we conclude that mitochondria are unlikely to be a direct target for benzimidazoles in stabilizing HIF-1α in normoxia.

Benzimidazoles affect HIF stabilization/activity through tubulin-binding activity

Another well-established and important target of antihelminthic benzimidazoles is tubulin (12, 25, 29). Antihelminthic benzimidazoles bind to tubulin and prevent its polymerization and subsequent formation of microtubules, although less robustly than classical microtubule depolymerizing agents (22) (Supplementary Fig. S2). Since microtubules are important

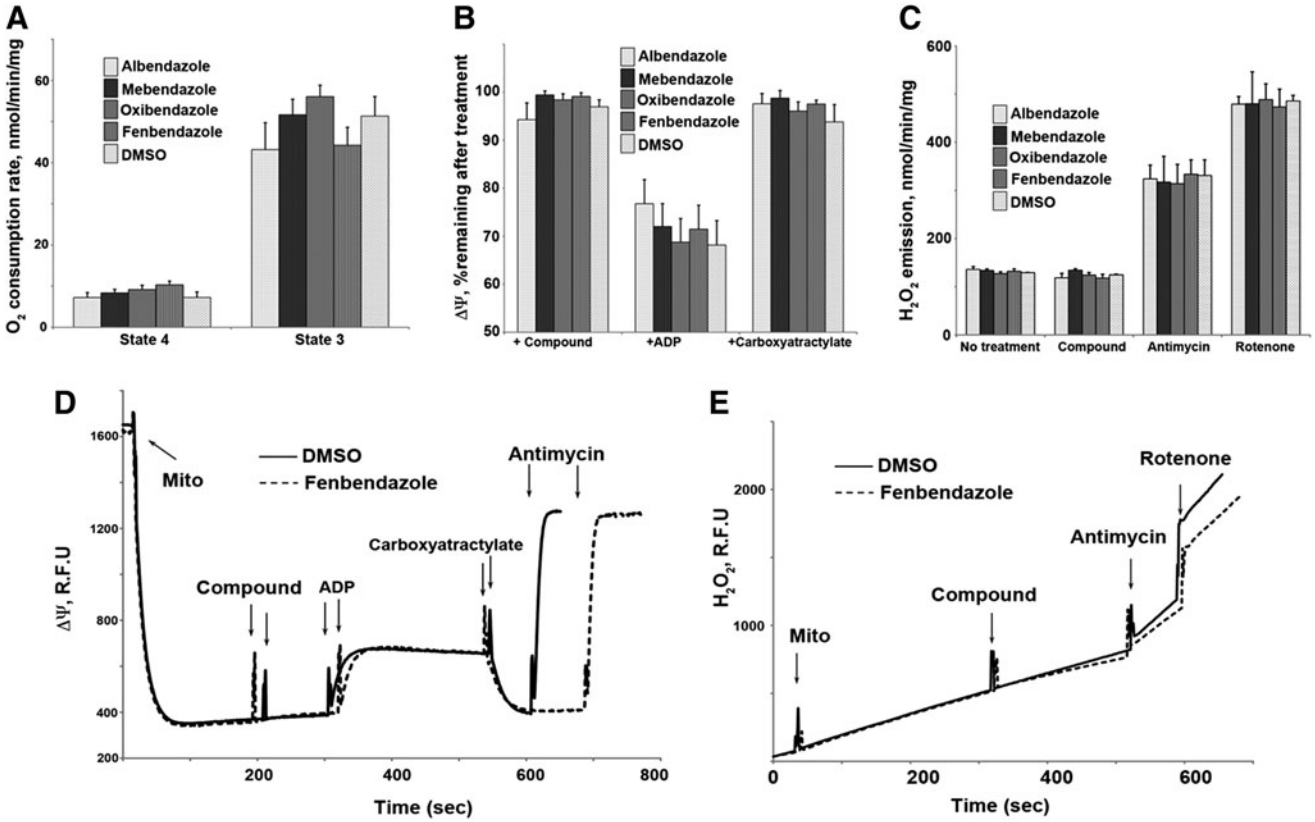

FIG. 3. Benzimidazoles have no effect on the respiration rates, the membrane potential changes, and ROS production of isolated mitochondria. (A) The respiration rates of mouse liver mitochondria. The incubation buffer and other conditions were as described in the Materials and Methods section. The compounds were added at 50 μM each before mitochondria. The non-phosphorylating respiration (State 4) was recorded for 2–3 min, and the phosphorylating respiration (State 3) was initiated by adding 400 nmol of ADP to the mitochondria suspension. **(B)** The membrane potential changes of mitochondria. The amplitude of the membrane potential remaining after adding the compounds, ADP, or carboxyatractylate is presented in percent of the total, taking the value of the membrane potential before adding the compounds as 100% and the value after antimycin addition as 0% (fully de-energized mitochondria). **(C)** ROS emission in response to benzimidazoles. The data are presented as average values of three experiments with standard errors. The data within the groups are not statistically different. **(D)** An example of the membrane potential test. The membrane potential was measured as described in the Materials and Methods section. Downward deflection of the curves means an increase in the membrane potential ($\Delta\Psi$). The compounds were added at 50 μM each where indicated. Other additions: ADP, 200 nmol ADP; carboxyatractylate (an inhibitor of ATP/ADP translocase) was added at 1 μM; antimycin (an inhibitor of Complex III of the respiratory chain) was added at 1 μg/ml. **(E)** An example of the ROS emission test. The ROS emission was measured as described in the Materials and Methods section. Upward deflection of the curves means an increase in the H_2O_2 in the incubation medium. The compounds were added at 50 μM each where indicated. Other additions: antimycin (an inhibitor of Complex III of the respiratory chain) was added at 1 μg/ml; rotenone (an inhibitor of Complex I of the respiratory chain) was added at 1 μM. The data are presented as average values of three to four experiments with standard errors of mean (±SEM). The differences within the groups are not statistically significant. ROS, reactive oxygen species.

cytoskeletal components, they are essential for neuron structure, growth, and axonal trafficking. Drugs and mutations that disrupt the dynamic equilibrium between free and polymerized tubulin may alter neuronal physiology, including cell-signaling pathways (7). In re-examining our hits (Table 1), we noted that colchicine, a prototypical tubulin-binding drug, also induced HRE-Luc activity to levels similar to benzimidazoles. To assess whether tubulin binding could be the on-target effect of benzimidazoles and colchicine in increasing HRE-Luc activity, we examined isocolchicine, a semi-synthetic structural isomer of colchicine with transposed C-ring carbonyl and methoxy groups. This structural modification decreases isocolchicine affinity for tubulin by 500-fold (16). Thus, if tubulin binding is an on-target effect, isocolchicine should not affect HRE-Luc activity at concentrations equimolar to colchicine. Indeed, while colchicine activated HRE-Luc in HT22 cells starting at 0.6 μM, isocolchicine had no effect (Fig. 4A). Based on this model, we predicted that other compounds which target the colchicine-binding site of tubulin would also induce reporter activity. Two such compounds, podophyllotoxin and nocodazole, were found to significantly increase HRE-Luc activity. Of note, we found that vinblastine, which depolymerizes microtubules by binding to a distinct site on β-tubulin, also activated the reporter in a dose-dependent manner. In contrast, Taxol, which stabilizes microtubules by binding to polymerized tubulin, had no effect (Fig. 4B). Consistent with these observations, colchicine, but not isocolchicine, increases ODD-Luc activity (Fig. 4C). This suggests that HIF-activation after treatment with tubulin-binding agents is through HIF-1α stabilization,

likely *via* the inhibition of prolyl hydroxylation. Taken together, these observations suggest that benzimidazoles, similar to other agents which bind monomeric tubulin, induce HIF-dependent gene expression under normoxia by stabilizing HIF-1α through an ODD-dependent mechanism.

Benzimidazoles and other agents that bind to tubulin protect embryonic cortical neurons against oxidative stress

To examine whether activation of the hypoxic adaptive response by benzimidazoles is associated with neuroprotection, we tested them in a glutathione depletion model of oxidative stress in immature primary neurons using the glutamate analog, homocysteic acid (HCA). Extracellular HCA inhibits cystine uptake by the system X_{c-} antiporter, and depletes intracellular glutathione by reducing its precursor, cysteine. This leads to the disruption of the oxidant-antioxidant balance in favor of oxidants and, ultimately, leads to cell death. Our lab and others have used this model to identify a number of novel pathways and drugs, including inhibitors of the HIF-PHDs, that have shown neuroprotection in preclinical models of acute and chronic neurodegeneration (3, 26, 30, 44, 52). We found that the tubulin-binding drugs colchicine and nocodozole protected neurons from HCA-induced oxidative stress (Fig. 5A, B, and D), while isocolchicine had no effect at the same concentrations (Fig 5C, D). Each benzimidazole identified in our screen protected neurons against oxidative stress in a dose-dependent manner (Fig. 6A–E). However, higher concentrations of benzimidazoles ($\geq 1\,\mu M$ for oxibendazole and $\geq 2\,\mu M$ for others) show a gradual negative impact on the basal viability. We also observed that while colchicine protects the soma during oxidative stress, it disrupts the neurites (Fig. 5D). To examine the effects of benzimidazoles on microtubule-dependent neuronal structures such as axons and dendrites, we stained embryonic cortical neurons after treatment with benzimidazoles with an antibody that recognizes a neuron-specific tubulin, βIII tubulin. Treatment with fenbendazole within the neuroprotective dose did not change the morphology of neurons (Fig. 7). Together, our data support a model in which tubulin-binding drugs, including benzimidazoles, activate hypoxic adaptation and show neuroprotective activity against oxidative stress without gross changes in neuronal morphology.

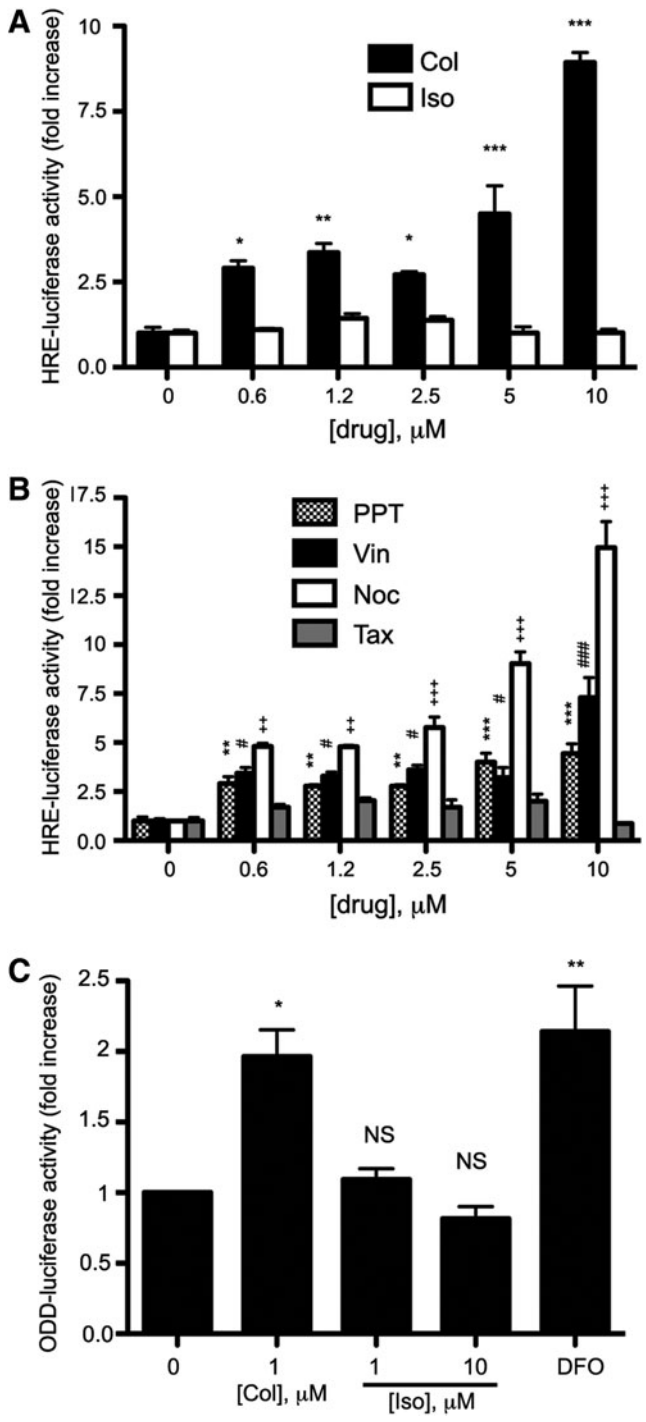

FIG. 4. Activation of markers of hypoxic adaptive response by tubulin-binding agents. (A) HT22 cells stably expressing HRE-Luc were treated with indicated concentrations of colchicine and isocolchicine. Isocolchicine is a structural isomer of colchicine that binds to tubulin with a much lower affinity. Colchicine increases HRE-luciferase activity, while isocolchicine does not (the difference of luciferase activity in Iso and vehicle-treated cells is not statistically significant at any dose). **(B)** Similar to colchicine, other tubulin-binding agents, including podophyllotoxin (PPT), vinblastine (Vin), and nocodazole (Noc), increase HRE-Luc expression; while taxol (Tax, which binds to and promotes microtubular stabilization) does not. The difference of luciferase activity in taxol and vehicle-treated cells is not statistically significant at any dose. **(C)** Colchicine increases the stability of the ODD-Luc reporter in HT22 cells at the dose of $1\,\mu M$, while isocolchicine has no effect at 1 or $10\,\mu M$. One hundred micromolar of DFO was used as a positive control. These findings suggest that tubulin-binding agents which classically destabilize microtubules and release free tubulin stabilize HIF and activate HIF-dependent gene expression similar to benzimidazoles. Quantifications of results are presented as the mean of three independent experiments ± SEM (*$p < 0.05$, **$p < 0.01$, and ***$p < 0.001$ [or each of corresponding symbols], one-way ANOVA with Dunnett multiple-comparison test).

Pretreatment with Taxol inhibits neuroprotective activity of tubulin-binding agents

If binding to free tubulin by benzimidazoles is necessary for the initiation of the signaling cascade that activates hypoxic adaptation and neuroprotection from oxidative stress,

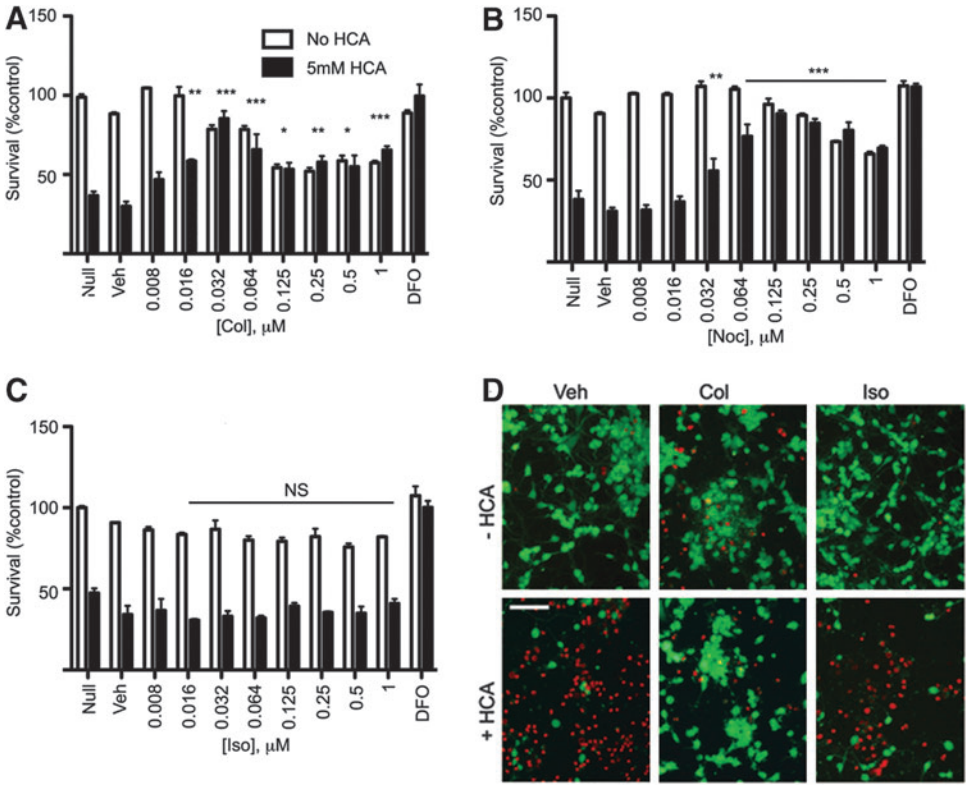

FIG. 5. Tubulin binding agents provide neuroprotection against oxidative stress. (A, B) Tubulin-binding agents colchicine (Col) and nocodazole (Noc) protect embryonic cortical neurons against oxidative stress induced by the glutamate analog, HCA. Glutamate or HCA inhibit cystine uptake, leading to depletion of the antioxidant, glutathione. **(C)** Isocolchicine (Iso) does not protect cortical neurons against oxidative stress at any of the tested concentrations. Survival for **(A–C)** was quantified by spectrophotometric assessment of the quantity of MTT converted to blue formazan. **(D)** Live-dead assay shows the micrograph of cultured neurons after treatment with 0.5 μM colchicine and isocolchicine with or without HCA. Quantifications of results are presented as the mean of three independent experiments ± SEM (*$p < 0.05$, **$p < 0.01$, and ***$p < 0.001$, one-way ANOVA with Dunnett multiple-comparison test). HCA, homocysteic acid.

then reduction of free tubulin should abrogate the protective actions of these drugs. To test the hypothesis, we first verified that Taxol reduces free tubulin levels in cortical neurons (Fig. 8A, B). We then pretreated primary neurons with 0.1 μM Taxol, 30 min before treatment with the tubulin-binding agents. This dose of Taxol does not cause significant neurotoxicity in cortical neurons (Fig. 8C). We used doses of tubulin-binding agents previously shown to provide maximum neuroprotection (Figs. 5 and 6). Taxol promotes microtubule stability, driving tubulin monomer into polymer (Fig. 8A); pretreatment with Taxol completely abrogated the neuroprotection conferred by tubulin-binding compounds, including benzimidazoles (Fig. 8C). To verify that reversal of protection was due to a specific effect of Taxol, we examined the effect of Taxol pretreatment on neuroprotection from HCA by an agent not known to bind tubulin, *N*-acetylcysteine (NAC). We have previously shown that NAC prevents glutathione depletion-induced death by enhancing intracellular glutathione levels (43). As expected, Taxol did not change the neuroprotective effect of NAC, suggesting that Taxol's ability to reverse protection is specific to that induced by drugs which bind to tubulin monomer. Moreover, the ability of Taxol to nullify both protective effects of classical tubulin binders and benzimidazoles is consistent with these agents working *via* a similar mechanism.

Mebendazole inhibits degradation of ODD-Luc, a surrogate marker of HIF activation, in vivo

Our findings suggested that benzimidazoles activate hypoxic adaptation and reduce oxidative death *in vitro*. However, one of the many challenges in translating the results of cell-based and invertebrate assays to more clinically relevant models in mammals is the unpredictable bioavailability of these compounds. Indeed, clear demonstration that the concentration of drug delivered safely to an animal affects a biomarker of drug activity studied in *in vitro* systems is essential. For example, benzimidazoles such as mebendazole are taken orally in clinical settings. The question remained as to whether oral mebendazole reaches sufficient concentrations to stabilize HIF-1α there. To evaluate HIF stabilization in the brain after treatment with these drugs, we used a transgenic mouse strain that ubiquitously expresses the HIF reporter ODD-Luc (47). We administered albendazole and mebendazole *via* oral gavage, daily for 5 days. After 6 h of the last dose, mice were anesthetized and then underwent live bioluminescence imaging using an IVIS-100 system. We observed that mebendazole, at a dose of 50 mg/kg, increased ODD-Luc activity fourfold in the brain compared with the control group (Fig. 9). By contrast to mebendazole (5), albendazole showed only a weak signal increase in the liver

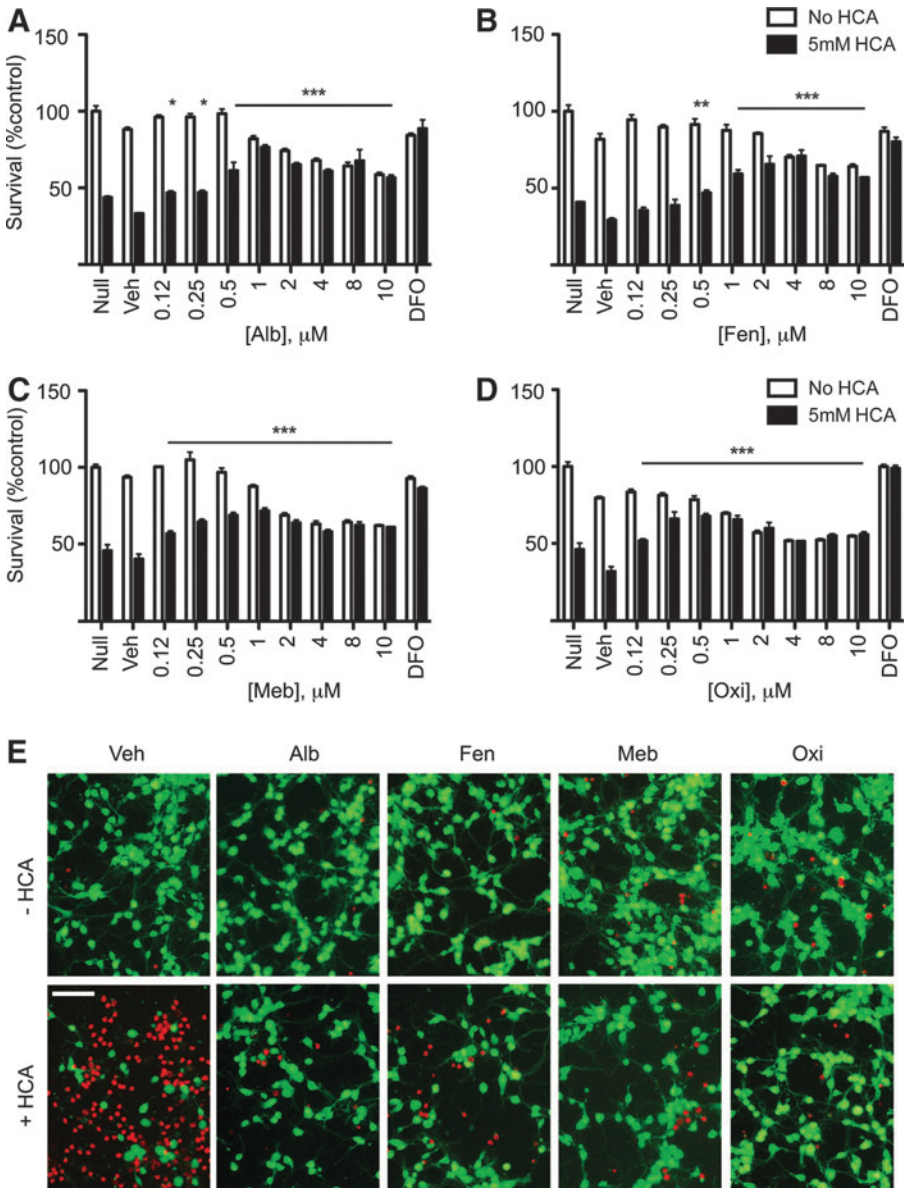

FIG. 6. Benzimidazoles protect cultured cortical neurons against oxidative stress. (A–D) All four clinically approved benzimidazoles protect embryonic cortical neurons from HCA-induced death. Neuronal survival was assessed by MTT assay. **(E)** Live-dead assay shows the micrograph of cultured neurons after treatment with 0.5 μM of benzimidazoles with or without HCA. Quantification of results is presented as the mean of three independent experiments ± SEM (*$p < 0.05$, **$p < 0.01$, and ***$p < 0.001$, one-way ANOVA with Dunnett-multiple comparison test).

with no detectable effect in the brain at a dose of 150 mg/kg (data not shown).

Discussion

Antihelminthic benzimidazoles are used throughout the world to treat parasitic infestations in a host of species and in diverse organs, including the central nervous system (CNS). An on-target effect of these agents is β-tubulin; specific mutations in this gene can confer resistance to antihelminthics (24). The study of the interaction of antihelminthic benzimidazoles with mammalian tubulin and its biological effect on the host, previously underappreciated, has developed into an area of growing interest. Indeed, two groups described the ability of benzimidazoles to modulate expression of PGC-1α, a co-activator involved in mitochondrial biogenesis, and to decrease ROS formation in non-neural cells (4, 58). Here, we expand our understanding of the host effects of benzimidazoles in neurons and show that these agents stabilize HIF-1α and augment HIF-dependent transcription. We correlate these changes with the ability of benzimidazoles to confer resistance to oxidative death in primary cortical neurons. Three lines of evidence suggest that free β-tubulin is targeted to achieve these biological effects. First, the effects of benzimidazoles on HIF-dependent gene expression and neuroprotection can be mimicked by structurally diverse agents that bind tubulin monomer, including those which interact with colchicine- or vinca alkaloid-binding sites. Second, the effects of colchicine on hypoxic adaptation and neuroprotection are abrogated by chemically modifying it to isocolchicine, which possesses a 500-fold lower affinity for tubulin than the parent compound. Third, reducing free tubulin levels with Taxol counteracts the protective effects of benzimidazoles.

Several models could explain the ability of drugs that bind β-tubulin to mimic hypoxia and prevent death in neurons. It is possible that these agents act to shift microtubule-tubulin equilibrium in favor of depolymerization, although we do not observe a gross change in neuronal architecture assessed by βIII

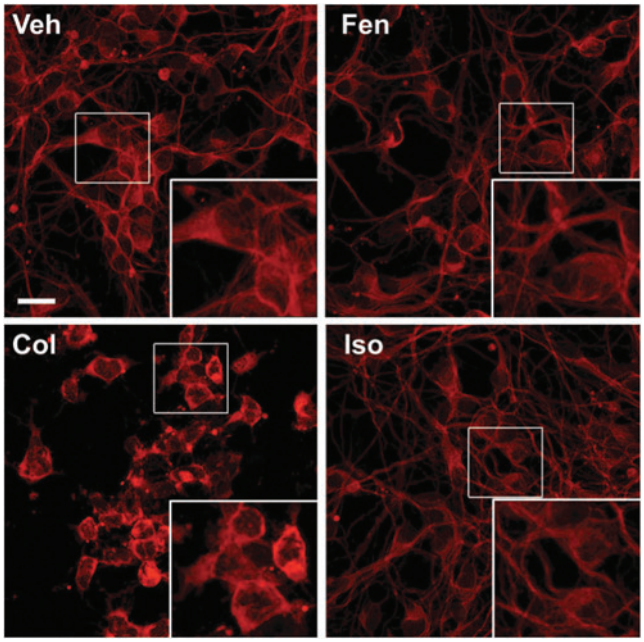

FIG. 7. Neuroprotective concentrations of antihelminthic benzimidazoles show no gross disruption of cortical neuron morphology. Immunocytochemical staining of embryonic cortical neurons at 16 h after treatment with 1 μM of fenbendazole using β-tubulin III antibody compared with colchicine (1 μM) and isocolchicine (1 μM) as positive and negative controls (scale bar = 25 μm, *insets* represent digitally magnified indicated area by 2×). To see this illustration in color, the reader is referred to the web version of this article at www.liebertpub.com/ars

tubulin staining in benzimidazole-treated neurons (Fig. 7). Small changes in microtubule dynamics are known to modulate signaling events that can lead to *de novo* transcription. For example, the cytoplasmic inhibitor of the transcription factor NF-κB, IκB can be sequestered by microtubules in the axonal initial segment. On microtubule depolymerization, IκB is degraded, unmasking the nuclear localization sequence of NF-κB and allowing it to translocate to the nucleus where it can up-regulate a number of genes, including HIF-1α (19). Increases in HIF-1α transcription could overwhelm the ability of neurons to degrade HIF-1α and lead to its stabilization. In this scheme, HIF-1α induction may be a biomarker of other genes that are known to abrogate oxidative stress, such as MnSOD (9), rather than being responsible for protection itself (49). Of course, it is also possible that benzimidazoles act post-transcriptionally rather than transcriptionally to enhance the interaction of HIF-1α (and other proteins) with Septins, a group of microtubule polymerizing guanine nucleotide-binding proteins which lead to HIF-1α stabilization in tumors (2). Since some of the earlier reports indicate that uptake and intracellular trafficking of iron and iron transporting proteins such as transferrin receptor and metal transporter protein 1 (MTP1) is microtubule dependent (34, 60), it is possible that benzimidazoles, through their tubulin-binding activity, might interrupt the intracellular trafficking of iron, an important cofactor for the activity of prolyl hydroxylases. Cytosolic iron starvation could lead to loss of HIF-PHD activity, stabilization of HIF, activation of HIF target genes, and HIF-independent neuroprotection (49, 50, 61).

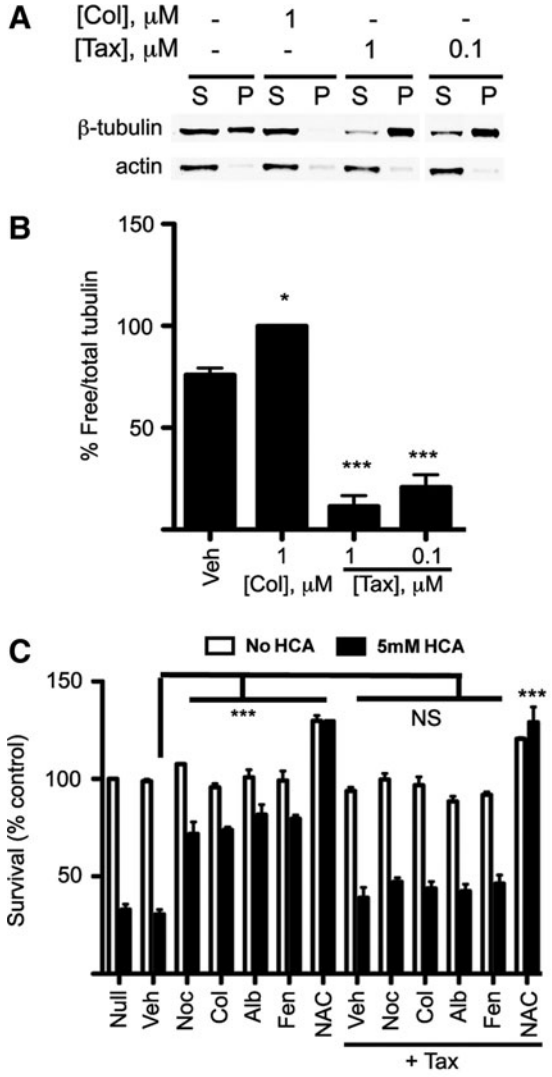

FIG. 8. Pretreatment with taxol abrogates the neuroprotective effects of tubulin-binding agents. (A) After 3 h of treatment with indicated concentrations of colchicine and taxol (Tax) in cultured embryonic neurons, free and polymerized tubulin, respectively, were monitored in the soluble (S) and insoluble (pellet, P) fractions, by immunoblotting with a β-tubulin-specific antibody. **(B)** Quantification of densitometry data from the three Western blot analyses shows that taxol significantly reduced the levels of free tubulin at both 1 and 0.1 μM doses. Since cortical neurons could tolerate 0.1 μM of taxol without significant toxicity (data not shown), we used this concentration for the pretreatment experiment. **(C)** As shown earlier, treatment with tubulin-binding agents, colchicine (0.03 μM), nocodazole (0.06 μM), and antihelminthic benzimidazoles (1 μM) protects neurons against glutathione depletion-induced death. Pretreatment with taxol (0.1 μM) for 30 min nullifies the neuroprotective effects of the tubulin-binding agents. The difference in the survival rate between vehicle and taxol-treated groups without HCA was statistically not significant. Quantifications of results are presented as the mean of three independent experiments ± SEM (*$p < 0.05$, and ***$p < 0.001$, one-way ANOVA with Dunnett multiple-comparison test).

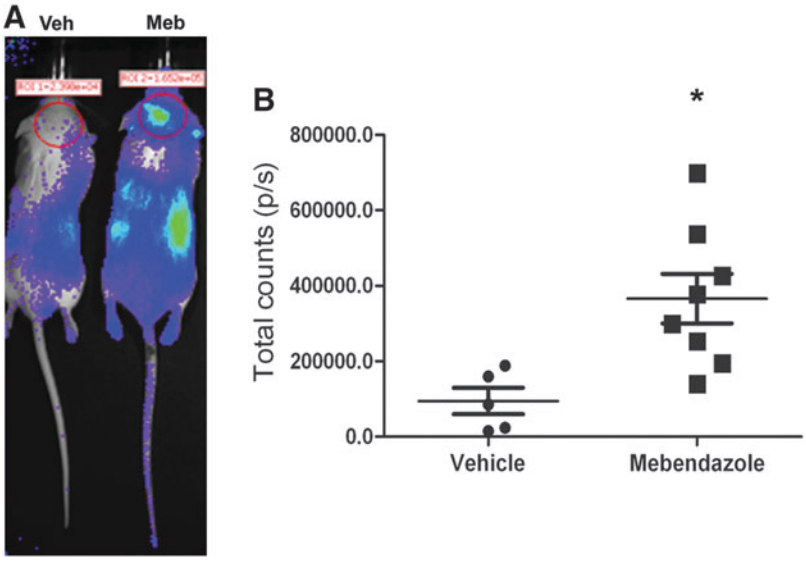

FIG. 9. Activation of the host hypoxic adaptive response *in vivo* after treatment with mebendazole. Mebendazole or vehicle was delivered to ODD-Luc mice through oral gavage at 50 mg/kg for 5 days. Six hours after the last dose, the animals were subjected to bioluminescence imaging using the IVIS 100 system **(A)**. The relative intensity of the luciferase activity of the ROI in head (marked as the *red circle*) was compared between vehicle ($n=5$) and mebendazole-treated ($n=8$) mice **(B)**. Quantifications of results are presented as the mean ± SEM ($^*p<0.05$, Student's *t*-test). ROI, region of interest.

The antihelminthic benzimidazoles are the first line treatment for parasitic infestations and are believed to be vermicidal by disrupting worm microtubules, leading to parasite immobility and death (57) without similarly affecting host cells. An unexplored possibility consistent with the results presented here is that host cells, unlike parasites, augment genetic adaptation in response to benzimidazole exposure that prevents extensive microtubular disruption. Indeed, a recent study shows that cytoskeletal insult through depolymerization of synaptic microtubules can lead to reduction of FOXO *via* activation of Akt to help limit microtubule disruption (39). Irrespective of the mechanism for selective toxicity in parasitic helminths by benzimidazoles, our findings show that they protect neurons in the nanomolar range. Finally, using a well-validated reporter, we demonstrate that mebendazole stabilized HIF-1α in the brain, a biomarker of hypoxic adaption. In clinics, the drug of choice to treat neurocysticercosis is albendazole. The concentration of its main metabolite, albendazole sulfoxide achieves levels in the brain that are sufficient to eradicate parasites (20). However, our finding that (i) albendazole sulfoxide is a weak neuroprotective agent compared with the parent compound (Supplementary Fig. S3), and (ii) albendazole failed to activate the HIF pathway in the brain, makes albendazole a less favorable therapeutic candidate than mebendazole in evaluating the effects of these agents on neurological conditions.

In addition to the novel potential applications for antihelminthic benzimidazoles, our studies also introduce numerous compounds with current clinical approval and short- and long-term safety data in humans that have the unexpected ability to activate hypoxic adaptation. A closer look at the list of our hits reveals at least two other groups of pharmacophores, isoflavones and phenylpropionic acids (ibuprofen and indoprofen). Of note, zomepirac, a non-steroidal anti-inflammatory drug, also a hit in our screen, binds to tubulin and mildly inhibits microtubular assembly (6). While the results of our primary screen have yet to be fully vetted, drugs such as hydralazine, atenolol, aminopyridine, and hydroxyzine with known applications in stroke prevention (11), functional recovery (10), or as CNS antihistamines (13) are of particular interest as novel activators of the adaptive program to hypoxia.

Materials and Methods

Chemicals

Albendazole, mebendazole, fenbendazole, oxibendazole, colchicine, nocodazole, citrate synthase and malic dehydrogenase, fumarase, oxaloacetic acid, acetyl-CoA, β-NADH, β-NAD, L-malic acid, fumaric acid, and DFO were purchased from Sigma and used without further purification.

Cell culture

Cortical neurons were harvested from E.15 CD-1 mouse embryos as previously described for rat cortical cultures (36). Dissociated neurons were plated in minimum essential media supplemented with glutamax, 10% fetal bovine serum (FBS), and 5% horse serum and seeded in 96-well (9×10^4 cells/well) or 6-well plates (2×10^6 cells/well), or 10 cm dishes (1×10^7 cells/dish) that were precoated with poly D-lysine. HT22 mouse hippocampal neuroblasts were cultured in Dulbecco's modified Eagle medium (Invitrogen) with high glucose, supplemented with glutamine, FBS (10%), and penicillin/streptomycin (Invitrogen).

ODD-luciferase activity

The ODD-luc construct encoded in pcDNA3.1 plasmid vector was constructed as previously described (47). Hydroxylation of prolines P402 and P564 within the HIF-1α ODD by HIF-PHDs permits binding to the VHL protein that targets it for proteasomal degradation. Targeted P402A and P564A mutation within the ODD prevents hydroxylation and confers stability to HIF-1α or the ODD-Luc construct under normoxia. ODD-Luc activity can, therefore, be used as a surrogate for HIF-1α stability regulated by the HIF-PHDs (47, 53). To make stably expressing ODD-Luc hippocampal mouse neuroblast HT22 cells, we co-transfected the plasmid construct along with a puromycin resistance plasmid (pBABEpuro). Transfected cells were grown in the presence of

4 μg/ml of puromycin. Luciferase activity was measured by luciferase assay kit (Promega) using an LMaxII™ microplate luminometer (Molecular Devices). ODD-Luciferase activity was normalized to the protein content of each well measured by bicinchoninic acid (BCA) protein assay (Pierce).

Neuronal viability assay

After 1 day in culture in 96-well plates, neurons were co-treated with an indicated concentration of each drug and homocysteic acid (HCA, 5 m*M*) to induce neuronal death *via* glutathione depletion (43). The compounds were solubilized in dimethyl sulfoxide (DMSO). To keep benzimidazoles soluble during serial dilution, we used 50% ethanol. The final concentration of ethanol in the culture media was 0.1%. For microtubule prestabilization experiments, the neurons were exposed to 100 n*M* of Taxol for 30 min before co-treatment with the compounds and HCA. Viability was assessed at 16 h after treatment by the MTT assay, or calcein AM/ethidium homodimer-1 staining (live-dead assay) (Invitrogen) under fluorescence microscopy according to the manufacturer's protocol. The viability has been calculated as the ratio of MTT absorbance in three treated wells divided by the average of three untreated wells in each plate and presented as percent to control.

Western blot analysis

Cells were plated in 10 cm plates, treated with the indicated compounds overnight, and then lysed with NP-40 buffer supplemented with protease inhibitors. For HIF-1α blots, nuclear proteins were enriched using a nuclear/cytoplasmic subcellular fractionation kit (Pierce). Protein content was measured by BCA protein assay (Pierce). Thirty microgram of total protein for $p21^{cip1/waf1}$ (p21) and 100 μg of nuclear protein for HIF-1α were loaded on 10% or 4%–12% gradient Bis-Tris polyacrylamide gels respectively (Invitrogen), resolved, and transferred to nitrocellulose membranes. Membranes were probed by antibodies against p21 (1:200; Santa Cruz), β-tubulin III (1:10,000; Epitomics), HIF-1α (1:500; Novus Biologicals), or histone H3 (1:1000; Cell Signaling Technology) and developed by IR-dye-conjugated antibodies (1:15,000) using the LI-COR system. Blots were imaged with the Odyssey IR quantitative Western blot detection system (LI-COR Biosciences).

Immunocytochemistry

Cortical neurons were treated with indicated compounds, fixed with 4% paraformaldehyde, and incubated with anti-β-tubulin III antibody (1:200; Epitomics), followed by secondary antibody as previously described (15).

Isolation of mitochondria

Non-synaptic mouse brain mitochondria were isolated by a modified isopycnic centrifugation procedure employing Percoll density gradient (32, 51). Briefly, cortex brain tissue was homogenized in the MSEGTA buffer composed of 225 m*M* mannitol, 75 m*M* sucrose, 20 m*M* HEPES (pH 7.4), 1 m*M* EGTA, and 0.2% (w/v) fatty acid-free bovine serum albumin (BSA) and centrifuged at 2000 $g \times 4$ min. The supernatant was collected and centrifuged at 12,000 $g \times 10$ min. The pellet was re-suspended in MSEGTA, layered over 25% (v/v) Percoll prepared in MSEGTA mixture, and centrifuged at 30,000 $g \times 10$ min. Purified mitochondria fraction was collected at the bottom of the tube, re-suspended in MSEGTA without added BSA, and washed twice by centrifugation at 12,000 $g \times 10$ min. Final mitochondrial pellet was re-suspended in MS buffer comprising 225 m*M* mannitol, 75 m*M* sucrose, and 20 m*M* HEPES (pH 7.4) and stored on ice. Protein content was estimated by a commercial BCA assay (Pierce Biotechnology/Thermo Scientific).

Mouse liver mitochondria were isolated by differential centrifugation. Liver was homogenized in MSEGTA buffer and centrifuged at 900 $g \times 10$ min; the supernatant was collected and centrifuged at 10,000 $g \times 10$ min; and the pellet was re-suspended in MSEGTA buffer with BSA omitted and centrifuged at 10,000 $g \times 10$ min. The final pellet was re-suspended in MSEGTA buffer without BSA to 15–20 mg mitochondria protein per milliliter and stored on ice during the experiment.

Functional assays

The base KEGTA incubation buffer employed in all assays was composed of 125 m*M* KCl, 20 m*M* HEPES (pH 7.2), 0.2 mg/ml BSA (fatty acid free), 4 m*M* KH_2PO_4, 0.2 m*M* EGTA, 5 m*M* glutamate, and 2 m*M* malate. For the measurements of the mitochondrial membrane potential, KEGTA was supplemented 2×10^{-6} *M* Safranine O. Mitochondria at 0.1–0.12 mg/ml were added to 1 ml of incubation buffer in a stirred thermostated ($t = 37$°C) cuvette, and the changes in the membrane potential were recorded by following the fluorescence of Safranine O with excitation and emission wavelengths of 495 and 586 nm, respectively, using a Hitachi 4500 (''Hitachi'') spectro-fluorimeter as described earlier (54, 55). For the measurements of mitochondrial ROS emission, KEGTA was supplemented with 4 U/ml of horseradish peroxidase, 40 U/ml of Cu, Zn superoxide dismutase, and 1×10^{-5} *M* Amplex RedUltra (Invitrogen). A change in the concentration of H_2O_2 in the medium was detected by fluorescence of the oxidized Amplex RedUltra product using excitation and emission wavelengths of 555 and 581 nm, respectively (54, 55). The response of Amplex RedUltra to H_2O_2 was calibrated by sequential additions of known amounts of H_2O_2. The concentration of commercial 30% H_2O_2 solution was calculated from light absorbance at 240 n*M* employing $E_{240} = 43.6\ M^{-1} \times cm^{-1}$; the stock solution was diluted to 0.1 m*M* with water and used for calibration immediately. The rates of resting and phosphorylating respiration were recorded with Oxytherm oximeter (Hansatech), at 37°C and 0.5–0.7 mg/ml of mouse liver mitochondria. All compounds were dissolved in DMSO at 25–50 m*M*.

Fumarase assay

Fumarate production from malate was measured with continuous monitoring of optical density at 240 nm, corresponding to the maximum absorption of fumarate ($E = 2440\ M^{-1} \times cm^{-1}$) in 0.1 *M* K-phosphate buffer, pH 7.6, in the presence of varied concentrations of benzimidazole and malate (0.05–0.4 m*M*). The data were plotted in a double-reciprocal format to compare inhibitory effects of various benzimidazoles, and on Dixon coordinates to determine the inhibition constant (K_i).

RNA extraction and real-time polymerase chain reaction

Cortical neurons were cultured in six-well plates and treated with indicated drugs. After 8 h, neurons were harvested with Trizol (Invitrogen). The levels of $p21^{cip1/waf1}$ (*cdkn1a*) mRNA were analyzed using One-step Taqman PCR assay mix and primers (Mm00432448_m1) on a 7500 Fast Real-Time PCR system (Applied Biosystems). β-Actin was used as an endogenous control (Mm00607939_s1).

Tubulin polymerization assay

The levels of free and polymerized tubulin were assessed at 3 h after treatment with indicated microtubule-binding agents using a microtubule/tubulin *in vivo* assay kit (Cytoskeleton).

Mebendazole treatment and in vivo *bioluminescence imaging*

Adult FVB.129S6-Gt(ROSA)26Sortm2(HIF1A/luc)Kael/J ODD Luc transgenic mice purchased from Jackson Laboratories were used to evaluate the inhibition of HIF-PHDs *in vivo*. For drug treatments, mebendazole tablets were powdered, mixed in a vehicle that was composed of phosphate-buffered saline and sesame oil 1:1 (Sigma), and delivered *via* oral gavage (100 μl) to adult ODD Luc mice. Animals were treated with mebendazole (50 mg/kg) or vehicle once a day for 5 days. Six hours after the last treatment, animals received an intraperitoneal injection of firefly D-luciferin potassium salt (75 mg/kg; i.p.) and were anesthetized with a mixture of 2.5% isoflurane and oxygen. The mice were placed in the chamber, where anesthesia was maintained with isoflurane 2%, administered through a nosecone *via* a gas anesthesia system. Luciferase luminescence was evaluated by a 100 Series IVIS Imaging System (Caliper Life Sciences, PerkinElmer). Mice were imaged on the dorsal side at 10 min post D-luciferin injection. The bioluminescent signal was integrated every 10 min for 40 min, with the peak signal observed at 20 min in most of the animals. Integral luminescence from a defined region of interest around each animal's brain was measured using the Living Image Software and expressed as photons per second of light.

Statistical analysis

Data were analyzed using Prism (GraphPad software). Quantitative data are presented as mean $\pm$ standard error of mean of at least three experiments. A comparison between the groups and control was performed by one-way analysis of variance (ANOVA), followed by *post hoc* Dunnett multiple-comparison test or Student's *t*-test for two-group analysis.

Acknowledgments

This work was supported by National Institutes of Health (P01 NIA AG014930, Project 1 to R.R.R.), the Dr. Miriam and Sheldon G. Adelson Program in Neurorehabilitation and Neural Repair, the Thomas Hartman Foundation for Parkinson's Research, the New York State Center of Research Excellence on Spinal Cord Injury, and the Burke Foundation. The authors wish to thank Dr. Natalia Smirnova for construction and evaluation of ODD-Luc reporter, Jimmy Payappilly and Dr. Hengchang Guo for providing technical assistance, and Dr. Gregg Gunderson for helpful scientific discussions.

Author Disclosure Statement

The authors declare no competing financial interests exist.

References

1. Aminova LR, Chavez JC, Lee J, Ryu H, Kung A, Lamanna JC, and Ratan RR. Prosurvival and prodeath effects of hypoxia-inducible factor-1alpha stabilization in a murine hippocampal cell line. *J Biol Chem* 280: 3996–4003, 2005.
2. Amir S, Wang R, Simons JW, and Mabjeesh NJ. SEPT9_v1 up-regulates hypoxia-inducible factor 1 by preventing its RACK1-mediated degradation. *J Biol Chem* 284: 11142–11151, 2009.
3. Aoyama K, Suh SW, Hamby AM, Liu J, Chan WY, Chen Y, and Swanson RA. Neuronal glutathione deficiency and age-dependent neurodegeneration in the EAAC1 deficient mouse. *Nat Neurosci* 9: 119–126, 2006.
4. Arany Z, Foo SY, Ma Y, Ruas JL, Bommi-Reddy A, Girnun G, Cooper M, Laznik D, Chinsomboon J, Rangwala SM, Baek KH, Rosenzweig A, and Spiegelman BM. HIF-independent regulation of VEGF and angiogenesis by the transcriptional coactivator PGC-1alpha. *Nature* 451: 1008–1012, 2008.
5. Bai RY, Staedtke V, Aprhys CM, Gallia GL, and Riggins GJ. Antiparasitic mebendazole shows survival benefit in 2 preclinical models of glioblastoma multiforme. *Neuro Oncol* 13: 974–982, 2011.
6. Bailey MJ, Worrall S, de Jersey J, and Dickinson RG. Zomepirac acyl glucuronide covalently modifies tubulin *in vitro* and *in vivo* and inhibits its assembly in an *in vitro* system. *Chem Biol Interact* 115: 153–166, 1998.
7. Bounoutas A, Kratz J, Emtage L, Ma C, Nguyen KC, and Chalfie M. Microtubule depolymerization in *Caenorhabditis elegans* touch receptor neurons reduces gene expression through a p38 MAPK pathway. *Proc Natl Acad Sci U S A* 108: 3982–3987, 2011.
8. Bruick RK and McKnight SL. A conserved family of prolyl-4-hydroxylases that modify HIF. *Science* 294: 1337–1340, 2001.
9. Dhar SK, Xu Y, and St Clair DK. Nuclear factor kappaB- and specificity protein 1-dependent p53-mediated bi-directional regulation of the human manganese superoxide dismutase gene. *J Biol Chem* 285: 9835–9846, 2010.
10. Domingo A, Al-Yahya AA, Asiri Y, Eng JJ, Lam T, and Spinal Cord Injury Rehabilitation Evidence Research Team. A systematic review of the effects of pharmacological agents on walking function in people with spinal cord injury. *J Neurotrauma* 29: 865–879, 2012.
11. Elewa HF, Kozak A, Johnson MH, Ergul A, and Fagan SC. Blood pressure lowering after experimental cerebral ischemia provides neurovascular protection. *J Hypertens* 25: 855–859, 2007.
12. Friedman PA and Platzer EG. Interaction of anthelmintic benzimidazoles and benzimidazole derivatives with bovine brain tubulin. *Biochim Biophys Acta* 544: 605–614, 1978.
13. Garcia-Gea C, Martinez-Colomer J, Antonijoan RM, Valiente R, and Barbanoj MJ. Comparison of peripheral and central effects of single and repeated oral dose administrations of bilastine, a new H1 antihistamine: a dose-range study in healthy volunteers with hydroxyzine and placebo

as control treatments. *J Clin Psychopharmacol* 28: 675–685, 2008.

14. Gonzalez FF, Abel R, Almli CR, Mu D, Wendland M, and Ferriero DM. Erythropoietin sustains cognitive function and brain volume after neonatal stroke. *Dev Neurosci* 31: 403–411, 2009.
15. Haskew-Layton RE, Payappilly JB, Smirnova NA, Ma TC, Chan KK, Murphy TH, Guo H, Langley B, Sultana R, Butterfield DA, Santagata S, Alldred MJ, Gazaryan IG, Bell GW, Ginsberg SD, and Ratan RR. Controlled enzymatic production of astrocytic hydrogen peroxide protects neurons from oxidative stress *via* an Nrf2-independent pathway. *Proc Natl Acad Sci U S A* 107: 17385–17390, 2010.
16. Hastie SB, Williams RC, Jr., Puett D, and Macdonald TL. The binding of isocolchicine to tubulin. Mechanisms of ligand association with tubulin. *J Biol Chem* 264: 6682–6688, 1989.
17. Isaacs JS, Jung YJ, Mole DR, Lee S, Torres-Cabala C, Chung YL, Merino M, Trepel J, Zbar B, Toro J, Ratcliffe PJ, Linehan WM, and Neckers L. HIF overexpression correlates with biallelic loss of fumarate hydratase in renal cancer: novel role of fumarate in regulation of HIF stability. *Cancer Cell* 8: 143–153, 2005.
18. Jin KL, Mao XO, and Greenberg DA. Vascular endothelial growth factor: direct neuroprotective effect in *in vitro* ischemia. *Proc Natl Acad Sci U S A* 97: 10242–10247, 2000.
19. Jung YJ, Isaacs JS, Lee S, Trepel J, and Neckers L. Microtubule disruption utilizes an NFkappa B-dependent pathway to stabilize HIF-1alpha protein. *J Biol Chem* 278: 7445–7452, 2003.
20. Jung-Cook H. Pharmacokinetic variability of anthelmintics: implications for the treatment of neurocysticercosis. *Expert Rev Clin Pharmacol* 5: 21–30, 2012.
21. Kaelin WG, Jr. and Ratcliffe PJ. Oxygen sensing by metazoans: the central role of the HIF hydroxylase pathway. *Mol Cell* 30: 393–402, 2008.
22. Kamal A, Kashi Reddy M, Shaik TB, Rajender, Srikanth YV, Santhosh Reddy V, Bharath Kumar G, and Kalivendi SV. Synthesis of terphenyl benzimidazoles as tubulin polymerization inhibitors. *Eur J Med Chem* 50: 9–17, 2012.
23. Knowles HJ, Tian YM, Mole DR, and Harris AL. Novel mechanism of action for hydralazine: induction of hypoxia-inducible factor-1alpha, vascular endothelial growth factor, and angiogenesis by inhibition of prolyl hydroxylases. *Circ Res* 95: 162–169, 2004.
24. Kwa MS, Veenstra JG, Van Dijk M, and Roos MH. Beta-tubulin genes from the parasitic nematode *Haemonchus contortus* modulate drug resistance in *Caenorhabditis elegans. J Mol Biol* 246: 500–510, 1995.
25. Lacey E. The role of the cytoskeletal protein, tubulin, in the mode of action and mechanism of drug resistance to benzimidazoles. *Int J Parasitol* 18: 885–936, 1988.
26. Langley B, D'Annibale MA, Suh K, Ayoub I, Tolhurst A, Bastan B, Yang L, Ko B, Fisher M, Cho S, Beal MF, and Ratan RR. Pulse inhibition of histone deacetylases induces complete resistance to oxidative death in cortical neurons without toxicity and reveals a role for cytoplasmic p21(waf1/cip1) in cell cycle-independent neuroprotection. *J Neurosci* 28: 163–176, 2008.
27. Li D, Bai T, and Brorson JR. Adaptation to moderate hypoxia protects cortical neurons against ischemia-reperfusion injury and excitotoxicity independently of HIF-1alpha. *Exp Neurol* 230: 302–310, 2011.
28. Linden T, Katschinski DM, Eckhardt K, Scheid A, Pagel H, and Wenger RH. The antimycotic ciclopirox olamine induces HIF-1alpha stability, VEGF expression, and angiogenesis. *FASEB J* 17: 761–763, 2003.
29. Lubega GW and Prichard RK. Specific interaction of benzimidazole anthelmintics with tubulin: high-affinity binding and benzimidazole resistance in Haemonchus contortus. *Mol Biochem Parasitol* 38: 221–232, 1990.
30. Ma C and D'Mello SR. Neuroprotection by histone deacetylase-7 (HDAC7) occurs by inhibition of c-jun expression through a deacetylase-independent mechanism. *J Biol Chem* 286: 4819–4828, 2011.
31. Majmundar AJ, Wong WJ, and Simon MC. Hypoxia-inducible factors and the response to hypoxic stress. *Mol Cell* 40: 294–309, 2010.
32. McConoughey SJ, Basso M, Niatsetskaya ZV, Sleiman SF, Smirnova NA, Langley BC, Mahishi L, Cooper AJ, Antonyak MA, Cerione RA, Li B, Starkov A, Chaturvedi RK, Beal MF, Coppola G, Geschwind DH, Ryu H, Xia L, Iismaa SE, Pallos J, Pasternack R, Hils M, Fan J, Raymond LA, Marsh JL, Thompson LM, and Ratan RR. Inhibition of transglutaminase 2 mitigates transcriptional dysregulation in models of Huntington disease. *EMBO Mol Med* 2: 349–370, 2010.
33. McCracken RO and Stillwell WH. A possible biochemical mode of action for benzimidazole anthelmintics. *Int J Parasitol* 21: 99–104, 1991.
34. Moriya M and Linder MC. Vesicular transport and apotransferrin in intestinal iron absorption, as shown in the Caco-2 cell model. *Am J Physiol Gastrointest Liver Physiol* 290: G301–G309, 2006.
35. Mu D, Chang YS, Vexler ZS, and Ferriero DM. Hypoxia-inducible factor 1alpha and erythropoietin upregulation with deferoxamine salvage after neonatal stroke. *Exp Neurol* 195: 407–415, 2005.
36. Murphy TH and Baraban JM. Glutamate toxicity in immature cortical neurons precedes development of glutamate receptor currents. *Brain Res Dev Brain Res* 57: 146–150, 1990.
37. Nagel S, Papadakis M, Chen R, Hoyte LC, Brooks KJ, Gallichan D, Sibson NR, Pugh C, and Buchan AM. Neuroprotection by dimethyloxalylglycine following permanent and transient focal cerebral ischemia in rats. *J Cereb Blood Flow Metab* 31: 132–143, 2011.
38. Nagel S, Talbot NP, Mecinovic J, Smith TG, Buchan AM, and Schofield CJ. Therapeutic manipulation of the HIF hydroxylases. *Antioxid Redox Signal* 12: 481–501, 2010.
39. Nechipurenko IV and Broihier HT. FoxO limits microtubule stability and is itself negatively regulated by microtubule disruption. *J Cell Biol* 196: 345–362, 2012.
40. Niatsetskaya Z, Basso M, Speer RE, McConoughey SJ, Coppola G, Ma TC, and Ratan RR. HIF prolyl hydroxylase inhibitors prevent neuronal death induced by mitochondrial toxins: therapeutic implications for Huntington's disease and Alzheimer's disease. *Antioxid Redox Signal* 12: 435–443, 2010.
41. Prass K, Scharff A, Ruscher K, Lowl D, Muselmann C, Victorov I, Kapinya K, Dirnagl U, and Meisel A. Hypoxia-induced stroke tolerance in the mouse is mediated by erythropoietin. *Stroke* 34: 1981–1986, 2003.
42. Prichard RK. Mode of action of the anthelminthic thiabendazole in *Haemonchus contortus. Nature* 228: 684–685, 1970.
43. Ratan RR, Murphy TH, and Baraban JM. Macromolecular synthesis inhibitors prevent oxidative stress-induced apoptosis in embryonic cortical neurons by shunting cysteine from protein synthesis to glutathione. *J Neurosci* 14: 4385–4392, 1994.
44. Ratan RR, Siddiq A, Aminova L, Lange PS, Langley B, Ayoub I, Gensert J, and Chavez J. Translation of ischemic

preconditioning to the patient: prolyl hydroxylase inhibition and hypoxia inducible factor-1 as novel targets for stroke therapy. *Stroke* 35: 2687–2689, 2004.
45. Ratan RR, Siddiq A, Aminova L, Langley B, McConoughey S, Karpisheva K, Lee HH, Carmichael T, Kornblum H, Coppola G, Geschwind DH, Hoke A, Smirnova N, Rink C, Roy S, Sen C, Beattie MS, Hart RP, Grumet M, Sun D, Freeman RS, Semenza GL, and Gazaryan I. Small molecule activation of adaptive gene expression: tilorone or its analogs are novel potent activators of hypoxia inducible factor-1 that provide prophylaxis against stroke and spinal cord injury. *Ann N Y Acad Sci* 1147: 383–394, 2008.
46. Ratan RR, Siddiq A, Smirnova N, Karpisheva K, Haskew-Layton R, McConoughey S, Langley B, Estevez A, Huerta PT, Volpe B, Roy S, Sen CK, Gazaryan I, Cho S, Fink M, and LaManna J. Harnessing hypoxic adaptation to prevent, treat, and repair stroke. *J Mol Med (Berl)* 85: 1331–1338, 2007.
47. Safran M, Kim WY, O'Connell F, Flippin L, Gunzler V, Horner JW, Depinho RA, and Kaelin WG, Jr. Mouse model for noninvasive imaging of HIF prolyl hydroxylase activity: assessment of an oral agent that stimulates erythropoietin production. *Proc Natl Acad Sci U S A* 103: 105–110, 2006.
48. Selak MA, Armour SM, MacKenzie ED, Boulahbel H, Watson DG, Mansfield KD, Pan Y, Simon MC, Thompson CB, and Gottlieb E. Succinate links TCA cycle dysfunction to oncogenesis by inhibiting HIF-alpha prolyl hydroxylase. *Cancer Cell* 7: 77–85, 2005.
49. Siddiq A, Aminova LR, Troy CM, Suh K, Messer Z, Semenza GL, and Ratan RR. Selective inhibition of hypoxia-inducible factor (HIF) prolyl-hydroxylase 1 mediates neuroprotection against normoxic oxidative death *via* HIF- and CREB-independent pathways. *J Neurosci* 29: 8828–8838, 2009.
50. Siddiq A, Ayoub IA, Chavez JC, Aminova L, Shah S, LaManna JC, Patton SM, Connor JR, Cherny RA, Volitakis I, Bush AI, Langsetmo I, Seeley T, Gunzler V, and Ratan RR. Hypoxia-inducible factor prolyl 4-hydroxylase inhibition. A target for neuroprotection in the central nervous system. *J Biol Chem* 280: 41732–41743, 2005.
51. Sims NR. Rapid isolation of metabolically active mitochondria from rat brain and subregions using Percoll density gradient centrifugation. *J Neurochem* 55: 698–707, 1990.
52. Sleiman SF, Langley BC, Basso M, Berlin J, Xia L, Payappilly JB, Kharel MK, Guo H, Marsh JL, Thompson LM, Mahishi L, Ahuja P, MacLellan WR, Geschwind DH, Coppola G, Rohr J, and Ratan RR. Mithramycin is a gene-selective Sp1 inhibitor that identifies a biological intersection between cancer and neurodegeneration. *J Neurosci* 31: 6858–6870, 2011.
53. Smirnova NA, Rakhman I, Moroz N, Basso M, Payappilly J, Kazakov S, Hernandez-Guzman F, Gaisina IN, Kozikowski AP, Ratan RR, and Gazaryan IG. Utilization of an *in vivo* reporter for high throughput identification of branched small molecule regulators of hypoxic adaptation. *Chem Biol* 17: 380–391, 2010.
54. Starkov AA. Measurement of mitochondrial ROS production. *Methods Mol Biol* 648: 245–255, 2010.
55. Starkov AA, Fiskum G, Chinopoulos C, Lorenzo BJ, Browne SE, Patel MS, and Beal MF. Mitochondrial alpha-ketoglutarate dehydrogenase complex generates reactive oxygen species. *J Neurosci* 24: 7779–7788, 2004.
56. Taylor CT and McElwain JC. Ancient atmospheres and the evolution of oxygen sensing *via* the hypoxia-inducible factor in metazoans. *Physiology (Bethesda)* 25: 272–279, 2010.
57. Vinaud MC, Ferreira CS, Lino Junior Rde S, and Bezerra JC. Taenia crassiceps: energetic and respiratory metabolism from cysticerci exposed to praziquantel and albendazole *in vitro*. *Exp Parasitol* 120: 221–226, 2008.
58. Wagner BK, Kitami T, Gilbert TJ, Peck D, Ramanathan A, Schreiber SL, Golub TR, and Mootha VK. Large-scale chemical dissection of mitochondrial function. *Nat Biotechnol* 26: 343–351, 2008.
59. Wang GL and Semenza GL. Purification and characterization of hypoxia-inducible factor 1. *J Biol Chem* 270: 1230–1237, 1995.
60. Wang X, Miller DS, and Zheng W. Intracellular localization and subsequent redistribution of metal transporters in a rat choroid plexus model following exposure to manganese or iron. *Toxicol Appl Pharmacol* 230: 167–174, 2008.
61. Zaman K, Ryu H, Hall D, O'Donovan K, Lin KI, Miller MP, Marquis JC, Baraban JM, Semenza GL, and Ratan RR. Protection from oxidative stress-induced apoptosis in cortical neuronal cultures by iron chelators is associated with enhanced DNA binding of hypoxia-inducible factor-1 and ATF-1/CREB and increased expression of glycolytic enzymes, p21(waf1/cip1), and erythropoietin. *J Neurosci* 19: 9821–9830, 1999.

Address correspondence to:
Prof. Rajiv R. Ratan
Burke-Cornell Medical Research Institute
785 Mamaroneck Avenue
White Plains, NY 10605

E-mail: rrr2001@med.cornell.edu

Date of first submission to ARS Central, August 23, 2013; date of final revised submission, April 11, 2014; date of acceptance, April 26, 2014.

Abbreviations Used

ANOVA = analysis of variance
BCA = bicinchoninic acid
BSA = bovine serum albumin
CMV = cytomegalovirus
CNS = central nervous system
DFO = deferoxamine
DMSO = dimethyl sulfoxide
EPO = erythropoietin
FBS = fetal bovine serum
HCA = homocysteic acid
HIF = hypoxia-inducible factor
HIF-PHD = HIF prolyl hydroxylase
HRE = hypoxia response element
MTP1 = metal transporter protein 1
NAC = *N*-acetylcysteine
ODD = oxygen-dependent degradation domain
ROI = region of interest
ROS = reactive oxygen species
SEM = standard error of mean
TCA = tricarboxylic acid
VEGF = vascular endothelial growth factor
VHL = Von Hippel-Lindau